②

NPS-63-88-006

# NAVAL POSTGRADUATE SCHOOL
## Monterey, California

SOLUTIONS TO THE SHALLOW WATER EQUATIONS
IN AN OCEAN BASIN FORCED BY UNSTEADY WINDS

by
MARY ALICE RENNICK
and
ROBERT L. HANEY

OCTOBER 1988

Report for the period
1 January 1986 to 30 June 1988

88 12 27 136

Naval Postgraduate School
Monterey, California  93943
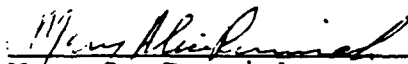
Admiral Robert C. Austin                     Harrison Shull
Superintendent                               Provost
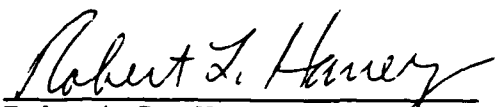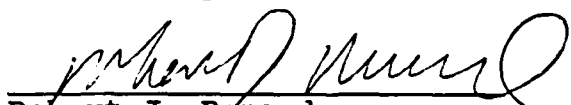
Reproduction of all or part of the report is authorized.

This report was prepared by:


_____                    _____
Mary A. Rennick                            Robert L. Haney
Adjunct Research Professor                 Professor of Meteorology




Reviewed by:                               Released by:


_____                    _____
Robert J. Renard                           Gordon E. Schacher
Chairman                                   Dean of Science and
Department of Meteorology                  Engineering

# REPORT DOCUMENTATION PAGE

| 1a REPORT SECURITY CLASSIFICATION | 1b RESTRICTIVE MARKINGS |
|---|---|
| Unclassified | |

| 2a SECURITY CLASSIFICATION AUTHORITY | 3 DISTRIBUTION/AVAILABILITY OF REPORT |
|---|---|
| | Unlimited |
| 2b DECLASSIFICATION/DOWNGRADING SCHEDULE | |

| 4 PERFORMING ORGANIZATION REPORT NUMBER(S) | 5 MONITORING ORGANIZATION REPORT NUMBER(S) |
|---|---|
| NPS-63-88-006 | |

| 6a NAME OF PERFORMING ORGANIZATION | 6b OFFICE SYMBOL (If applicable) | 7a NAME OF MONITORING ORGANIZATION |
|---|---|---|
| Naval Postgraduate School | Code 63 | Dr. Hassan Virji |

| 6c ADDRESS (City, State, and ZIP Code) | 7b ADDRESS (City, State, and ZIP Code) |
|---|---|
| Department of Meteorology Naval Postgraduate School Monterey, CA 93943 | Climate Dynamics Program National Science Foundation Washington, D.C. 20550 |

| 8a NAME OF FUNDING/SPONSORING ORGANIZATION | 8b OFFICE SYMBOL (If applicable) | 9 PROCUREMENT INSTRUMENT IDENTIFICATION NUMBER |
|---|---|---|
| National Science Foundation | | |

| 8c ADDRESS (City, State and ZIP Code) | 10 SOURCE OF FUNDING NUMBERS | | | |
|---|---|---|---|---|
| Washington, D.C. 20550 | PROGRAM ELEMENT NO | PROJECT NO ATM-8514012 | TASK NO | WORK UNIT ACCESSION NO |

11 TITLE (Include Security Classification)

Solutions to Shallow Water Equations in an Ocean Basin Forced by Unsteady Winds

12 PERSONAL AUTHOR(S)
M.A. Rennick and R.L. Haney

| 13a TYPE OF REPORT | 13b TIME COVERED | 14 DATE OF REPORT (Year Month Day) | 15 PAGE COUNT |
|---|---|---|---|
| Technical | FROM 1/1/86 TO 30/6/88 | October 13, 1988 | 31 |

16 SUPPLEMENTARY NOTATION

| 17 | COSATI CODES | | 18 SUBJECT TERMS (Continue on reverse if necessary and identify by block number) |
|---|---|---|---|
| FIELD | GROUP | SUB-GROUP | |
| | | | |

19 ABSTRACT (Continue on reverse if necessary and identify by block number)
The analytic solution to the shallow water equations in a closed equatorial basin subject to arbitrary wind forcing is presented. Two particular examples including the transient response of the basin to a moving "top-hat" wind pulse representative of the atmospheric Southern Oscillation, are worked out in detail. The analytic results compare favorably with previously published numerical model results and offer new potential for interpreting equatorial ocean variability—both modeled and observed.

| 20 DISTRIBUTION/AVAILABILITY OF ABSTRACT | 21 ABSTRACT SECURITY CLASSIFICATION |
|---|---|
| ☐ UNCLASSIFIED/UNLIMITED  ☒ SAME AS RPT  ☐ DTIC USERS | |

| 22a NAME OF RESPONSIBLE INDIVIDUAL | 22b TELEPHONE (Include Area Code) | 22c OFFICE SYMBOL |
|---|---|---|
| Mary A. Rennick | (408) 646-2516 | |

DD FORM 1473, 84 MAR      83 APR edition may be used until exhausted     
All other editions are obsolete

# Solutions to the Shallow Water Equations in an

# Ocean Basin Forced by Unsteady Winds

M. A. Rennick and R. L. Haney

Naval Postgraduate School, Monterey, CA 93943

October 13, 1988

## Abstract

The analytic solution to the shallow water equations in a closed equatorial basin subject to arbitrary wind forcing is presented. Two particular examples, including the transient response of the basin to a moving "top-hat" wind pulse representative of the atmospheric Southern Oscillation, are worked out in detail. The analytic results compare favorably with previously published numerical model results and offer new potential for interpreting equatorial ocean variability–both modeled and observed.

# List of Figures

# List of Tables

Acknowledgements

1

# 1 Introduction

The collective atmosphere-ocean anomaly known as the El Niño–Southern Oscillation (ENSO) has received a great deal of attention in recent years. One common framework within which the system has been studied is the shallow water equations. With this approach, the atmosphere and/or the ocean is treated as the first baroclinic mode of the shallow water equations. The equations governing the two systems are the same, except for their equivalent depths (or phase speeds) and their forcing functions. The atmosphere is generally forced by a source term in the continuity equation, representing heating at middle to upper levels of the atmosphere; the ocean is usually forced by a momentum source, representing surface wind stress.

Shallow water models of an equatorial ocean basin have been solved numerically by Hurlburt et. al.(1976), Busalacchi and O'Brien (1981), Busalacchi, et. al. (1983), Weisburg and Tang (1983), and others, using both hypothetical and observed forcing functions to represent enhanced surface wind stress due to anomalous westerly wind events. McCreary (1976), Cane and Sarachik (1976), Cane and Sarachik (1981), Cane (1979), McCreary and Lukas (1986), and others obtained analytic solutions to similar sets of equations. Similar techniques have been used by Gill (1980), among others, to investigate the response of the first baroclinic mode of the global atmosphere to heating due to enhanced convection associated with sea surface temperature anomalies in the equatorial Pacific.

An obvious extension of these studies has involved the coupling of the atmospheric and oceanic shallow water models through the introduction of interactive forcing functions. The resulting interactive models have more degrees of freedom than the individual component models, and they provide additional insight regarding possible interdependencies and resonances of the coupled ocean-atmosphere system. Normal mode solutions to such coupled (but laterally unbounded) systems were studied by Lau (1981), Philander et. al.(1984), Yamagata (1985), Rennick and Haney (1986), and Hirst (1986), all of whom found the possibility of unstable interactions under different sets of somewhat restrictive assumptions. Numerical solutions to the coupled equations have been studied under fewer restrictions by Rennick (1983), Schopf and Suarez (1988), and Hirst (1988).

One feature of most of the analytic studies cited above is that they failed to account for the effects of reflections at the eastern and western boundaries of the ocean basin. The ocean response study of McCreary and Lukas (1986), and all the normal mode studies of the coupled system noted above, effectively treated an unbounded equatorial ocean band, with no continents. However, the numerical studies, as well as thecretical work by McCalpin (1988), have shown that boundary reflections play an important role in partitioning energy among Kelvin and Rossby modes, and thereby affecting the structure of disturbances, and the energy available to the unstable modes. In addition, observational evidence presented by White, et. al. (1985) suggests that reflection from the western boundary in the ocean is important during ENSO events.

In this work, the forced shallow water equations are solved analytically in a closed equa-

torial oce _n basin using a method of solution quite similar to that used by McCreary (1976). Some of McCreary's simplifying assumptions were dropped, requiring a final numerical step to construct the solutions, and a wider range of forcing functions was investigated. The problem was posed as an initial value problem. The time dependence was made algebraic by a Laplace transform. The dependent variables were expanded with respect to latitude in terms of the Hermite polynomials, and the resulting system was reduced to a single equation for $\hat{u}_n(s, x)$, the transform of the Hermite coefficients for the zonal current. Finally, the solution was back-transformed to physical space numerically, and the total solution was reconstructed.

Section 2 reviews the system of equations and the method of solution. The results obtained using two different forcing functions are described in Section 3. Some final comments on the solutions are included in Section 4.

## 2  Basic Formulation

In order to find the response of the ocean basin to prescribed forcing, the shallow water equations on the equatorial $\beta$ plane are written in their dimensional form:

$$g\frac{\partial h}{\partial \tilde{x}} + \frac{\partial u}{\partial \tilde{t}} - \beta \tilde{y} v = \tau$$

$$g\frac{\partial h}{\partial \tilde{y}} + \beta \tilde{y} u + \frac{\partial v}{\partial \tilde{t}} = 0$$

$$\frac{\partial h}{\partial \tilde{t}} + d\frac{\partial u}{\partial \tilde{x}} + d\frac{\partial v}{\partial \tilde{y}} = 0$$

where $\tau$ is the surface wind stress, d is the mean depth of the fluid, and the other variables have their usual meanings. The independent variables are nondimensionalized according to

$$t = \beta^{\frac{1}{2}} c^{\frac{1}{2}} \tilde{t}$$

$$x = \beta^{\frac{1}{2}} c^{-\frac{1}{2}} \tilde{x}$$

$$y = \beta^{\frac{1}{2}} c^{-\frac{1}{2}} \tilde{y}$$

where $c \equiv (gd)^{\frac{1}{2}}$. The fundamental equations for the system are then

$$\frac{g}{c} h_x + u_t - yv = \beta^{-\frac{1}{2}} c^{-\frac{1}{2}} \tau \tag{1}$$

$$\frac{g}{c} h_y + yu + v_t = 0 \tag{2}$$

$$\frac{g}{c} h_t + u_x + v_y = 0 \tag{3}$$

The zonal current is required to vanish at the ends of the basin $(x = 0, l)$, and the meridional current is required to vanish far from the equator. Initially, the system is at

rest, with a flat surface. These boundary and initial conditions are expressed as

$$u(0, x, y) = 0 \tag{4}$$

$$v(0, x, y) = 0 \tag{5}$$

$$h(0, x, y) = 0 \tag{6}$$

$$u = 0 \quad \text{at} \quad x = 0, l \tag{7}$$

$$v \to 0 \quad \text{as} \quad y \to \pm\infty \tag{8}$$

The values of the constants are shown in Table 1.

A Laplace transform of (1)–(3) gives

$$\frac{g}{c}\hat{h}_x + s\hat{u} - y\hat{v} = \beta^{-\frac{1}{2}}c^{-\frac{1}{2}}\hat{\tau} \tag{9}$$

$$\frac{g}{c}\hat{h}_y + y\hat{u} + s\hat{v} = 0 \tag{10}$$

$$\frac{g}{c}s\hat{h} + \hat{u}_x + \hat{v}_y = 0 \tag{11}$$

where $\hat{\xi}(s, x, y) = \mathcal{L}(\xi) = \int_0^\infty \xi(t, x, y)e^{-st}dt$. $\hat{h}$ is eliminated by taking $s(9) - (11)_x$ and $s(10) - (11)_y$.

$$s^2\hat{u} - \hat{u}_{xx} - ys\hat{v} - \hat{v}_{xy} = \beta^{-\frac{1}{2}}c^{-\frac{1}{2}}s\hat{\tau} \tag{12}$$

$$ys\hat{u} - \hat{u}_{xy} + s^2\hat{v} - \hat{v}_{yy} = 0 \tag{13}$$

The dependent variables and the forcing function are expressed as sums of the Hermite polynomials, $H_n$.

$$\hat{\xi}(s, x, y) = \sum_{n=0}^\infty \hat{\xi}_n(s, x)H_n(y)e^{-y^2/2}$$

6

| | dimensional value | nondimensional value |
|---|---|---|
| $g$ | 9.8 m s$^{-2}$ | |
| $d$ | .408 m | |
| $c$ | 2.0 m s$^{-1}$ | |
| $l$ | 14780 km | 50 |
| $\beta^{\frac{1}{2}}c^{\frac{1}{2}}$ | $6.767 \times 10^{-6}$ s$^{-1}$ | |
| $\beta^{\frac{1}{2}}c^{-\frac{1}{2}}$ | $3.383 \times 10^{-6}$ m | |
| $t_0$ | 34.2 days | 20 |
| $\gamma$ | .0667 | .0667 |
| $a$ | .00835 day$^{-1}$ | .0143 |
| $\eta$ | .358 m s$^{-1}$ | .179 |
| $\lambda$ | 7390 km | 25 |

Table 1: Values of constants

7

Expanding (12) and (13) in terms of $H_n$, multiplying by $H_m\,e^{-v^2/2}$ and integrating over $y$, a pair of equations for $\hat{u}_n$ and $\hat{v}_n$ are obtained.

$$(s^2 - D^2)\hat{u}_n - (n+1)(s+D)\hat{v}_{n+1} - \frac{1}{2}(s-D)\hat{v}_{n-1} \;=\; \beta^{-\frac{1}{2}}c^{-\frac{1}{2}}s\hat{T}_n \quad (14)$$

$$(n+1)(s-D)\hat{u}_{n+1} + \frac{1}{2}(s+D)\hat{u}_{n-1}$$

$$-(n+2)(n+1)\hat{v}_{n+2} + (s^2 + n + \frac{1}{2})\hat{v}_n - \frac{1}{4}\hat{v}_{n-2} \;=\; 0 \quad\quad (15)$$

These equations are rewritten in matrix form

$$A|\hat{u}\rangle - B|\hat{v}\rangle \;=\; C|\hat{\tau}\rangle$$

$$E|\hat{u}\rangle + F|\hat{v}\rangle \;=\; 0$$

where

$$A_{n,m} \;=\; (s^2 - D^2)\delta_{n,m}$$

$$B_{n,m} \;=\; \frac{1}{2}(s-D)\delta_{n,m+1} + (n+1)(s+D)\delta_{n,m-1}$$

$$C_{n,m} \;=\; \beta^{-\frac{1}{2}}c^{-\frac{1}{2}}s\delta_{n,m}$$

$$E_{n,m} \;=\; \frac{1}{2}(s+D)\delta_{n,m+1} + (n+1)(s-D)\delta_{n,m-1}$$

$$F_{n,m} \;=\; -\frac{1}{4}\delta_{n,m+2} + (s^2 + n + \frac{1}{2})\delta_{n,m} - (n+2)(n+1)\delta_{n,m-2}$$

and $D = \frac{\partial}{\partial x}$. The matrix operators $A$, $B$, $C$, $E$, and $F$ are all linear, with constant coefficients. Then $FB - BF = 0$, and

$$(FA + BE)|\hat{u}\rangle = FC|\hat{\tau}\rangle \quad\quad (16)$$

8

The operators in (16) are expanded

$$(FA + BE) = -\tfrac{1}{4}(s^2 - D^2)\delta_{n,m+2} \quad +s^2 + n + \tfrac{1}{2}(s^2 - D^2)\delta_{n,m} \quad -(n+2)(n+1)(s^2 - D^2)\delta_{n,m}$$

$$+\tfrac{1}{4}(s^2 - D^2)\delta_{n,m+2} \quad +\tfrac{1}{2}n(s-D)^2\delta_{n,m}$$

$$+\tfrac{1}{2}(n+1)(s+D)^2\delta_{n,m} \quad +(n+1)(n+2)(s^2 - D^2)\delta_{n,m}$$

$$FC = \beta^{-\frac{1}{2}}c^{-\frac{1}{2}}s\left\{-\tfrac{1}{4}\delta_{n,m+2} \quad +(s^2 + n + \tfrac{1}{2})\delta_{n,m} \quad -(n+2)(n+1)\delta_{n,m-2}\right\}$$

The off diagonal terms of $(FA + BE)$ all cancel, so that (16) may be written

$$\left\{s^2 D^2 + sD + (s^2 + 2n + 1)s^2\right\}\hat{u}_n = \beta^{-\frac{1}{2}}c^{-\frac{1}{2}}s\left\{-\frac{1}{4}\hat{\tau}_{n-2} + (s^2 + n + \frac{1}{2})\hat{\tau}_n - (n+2)(n+1)\hat{\tau}_{n+2}\right\}$$

$$(17)$$

General solutions to (17) are constructed as the sum of two parts, $\hat{u}_n = \hat{U}_n + \hat{v}_n$, where $\hat{U}_n$ is a particular solution depending on the forcing, and $\hat{v}_n$ is a solution to the homogeneous form of the equation. Solutions to the homogeneous equation are given by $\hat{v}_n = \hat{f}_n(s)e^{k_n(s)}$, where $f_n$ is an arbitrary function of $s$ (to be determined by the boundary conditions), and $k_n(s)$ is given by the dispersion relation

$$-s^2 k^2 + sk + (s^2 + 2n + 1)s^2 = 0$$

$$k_n^{\pm} = -\frac{1}{2s}\left[-1 \pm \sqrt{1 + 4s^2(s^2 + 2n + 1)}\right] \qquad (18)$$

The Hermite representation guarantees that the solution will vanish as $y \to \pm\infty$. The boundary conditions at $x = 0, l$ must be satisfied by an appropriate choice of $\hat{f}_n(s)$. That is, the $\hat{f}_n(s)$ must be chosen such that

$$\hat{f}_n^+(s) + \hat{f}_n^-(s) + \hat{U}_n(s,0) = 0$$

$$\hat{f}_n^+(s)\,e^{k_n^+ l} + \hat{f}_n^-(s)\,e^{k_n^- l} + \hat{U}_n(s,l) = 0$$

9

Thus, the coeficients $f_n^\pm(s)$ are given by

$$\hat{f}_n^\pm(s) = \mp \frac{\hat{U}_n(s,l) - e^{k_n^\mp l}\hat{U}_n(s,0)}{e^{k_n^+ l} - e^{k_n^- l}} \tag{19}$$

General solutions to (17) which satisfy both initial and boundary conditions are then found for different forcing functions $\tau(t,x,y)$, and back transformed to physical space.

# 3 Solutions

## a  Zonally uniform forcing

The first case which was investigated was driven by a simple wind stress function

$$\tau(t, x, y) = \frac{A}{t_0} \left[ t\Theta(t) - (t - t_0)\Theta(t - t_0) \right] e^{-\frac{1}{2}\gamma\psi^2} \tag{20}$$

where $\Theta$ is the Heavyside step function. (20) represents a zonally uniform eastward wind stress with a Gaussian meridional profile. The width of the Gaussian corresponds to that of a first meridional mode atmospheric Kelvin wave. The magnitude of the forcing increased from zero to a finite value corresponding to a uniform westerly wind anomaly of about 10 m s$^{-1}$ over a period of about one month. This uniform "spin-up" forcing is very similar to that used by McCreary (1976).

The above forcing was expanded in terms of Hermite polynomials, and each term was Laplace transformed to yield

$$\hat{\tau}_n = \frac{1}{s^2 t_0} \left[ 1 - e^{-st_0} \right] \mathcal{T}_n$$

where $\mathcal{T}_n$ is the $n^{th}$ Hermite coefficient of $Ae^{-\frac{1}{2}\gamma\psi^2}$. Particular solutions to (17) are

$$\hat{U}_n(s, x) = \frac{\beta^{-\frac{1}{2}} c^{-\frac{1}{2}}}{s^3(s^2 + 2n + 1)} \frac{1 - e^{-st_0}}{t_0} \left[ -\frac{1}{4}\mathcal{T}_{n-2} + (s^2 + n + \frac{1}{2})\mathcal{T}_n - (n + 2)(n + 1)\mathcal{T}_{n+2} \right]$$

Using (19), the general solution for $\hat{u}_n$ is found to be

$$\hat{u}_n(s, x) = \hat{U}_n(s, x) - \frac{\left[ \hat{U}_n(s, l) - e^{k_n^- l}\hat{U}_n(s, 0) \right] e^{k_n^+ x} - \left[ \hat{U}_n(s, l) - e^{k_n^+ l}\hat{U}_n(s, 0) \right] e^{k_n^- x}}{e^{k_n^+ l} - e^{k_n^- l}} \tag{21}$$

11

The Hermite series for $\tau(y)$ is truncated at $n = 6$, and solutions are found for $\hat{u}_n(s, x)$. These are back transformed numerically, using the IMSL subroutine INLAP, and the solution for $u(t, x, y)$ is reconstructed in physical space.

The zonal current anomaly for this case is shown in Figs. 1 and 2. These figures show an initial response of eastward current anomalies along the equator in response to the eastward stress anomaly. By $t = 5$ (roughly 8.5 days) this response is limited to a narrow latitude band along the equator, with a wider region of eastward flow near the eastern end of the basin. The strongest response at this time is the .20 m s$^{-1}$ westward currents located on the equator near the western end of the basin. Less intense westward currents flank the eastward equatorial flow across most of the basin, with eastward return flow at higher latitudes.

At $t = 20$ ($\approx$ 34 days) the forcing has reached its final value. The equatorial currents are now westward at all longitudes, with a maximum of .18 m s$^{-1}$across most of the basin. The patch of enhanced westward flow near the western boundary is still evident, but its magnitude has decreased to about .14 m s$^{-1}$. Under the influence of continued forcing, the same general pattern persists. The meridional extent of the westward currents continues to expand with time and the relative magnitudes of the eastern and western current maxima change so that at $t = 100$ ($\approx$ 171 days) they are both $\approx$ 1.6 m s$^{-1}$(Fig. 2).

Only the far western part of the basin has reached a steady state configuration at this time. Examination of the Hermite coefficients (not shown) indicates that only the $n = 0$ term has reached a steady state value. The $n = 2$ term has equilibrated over the western
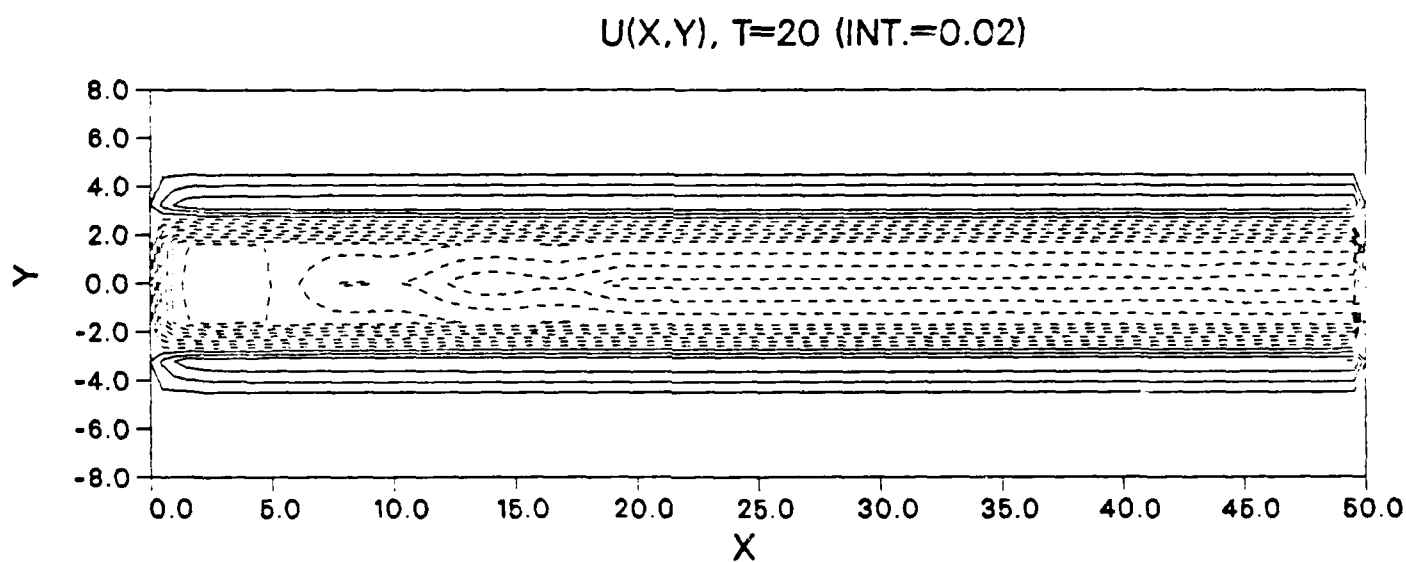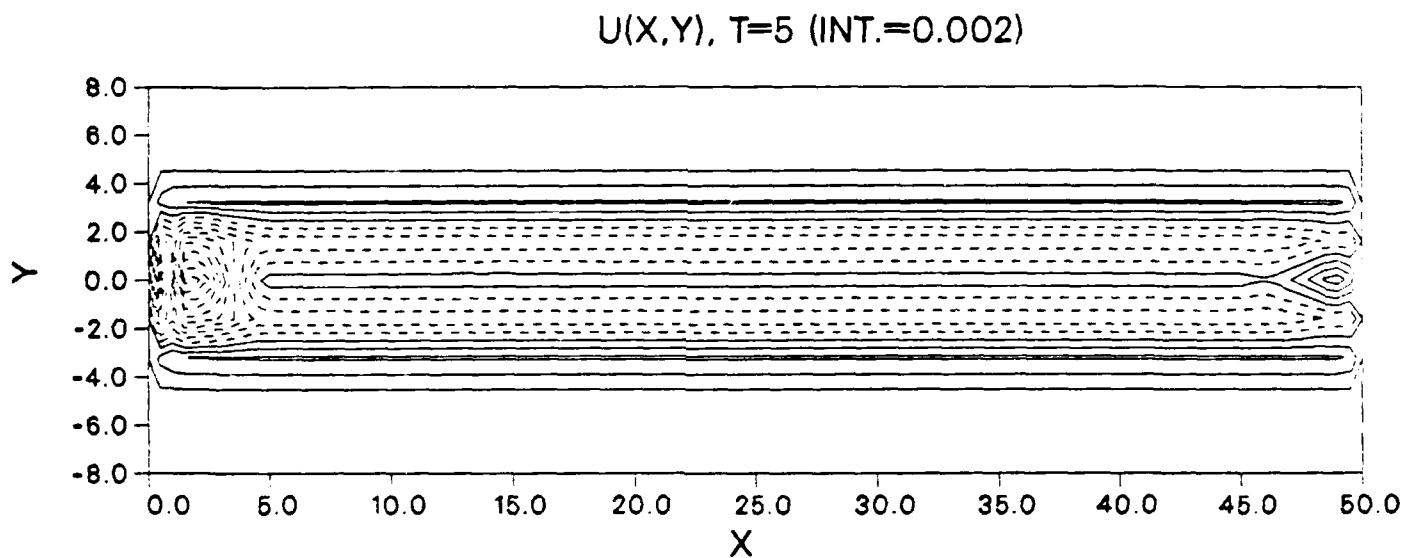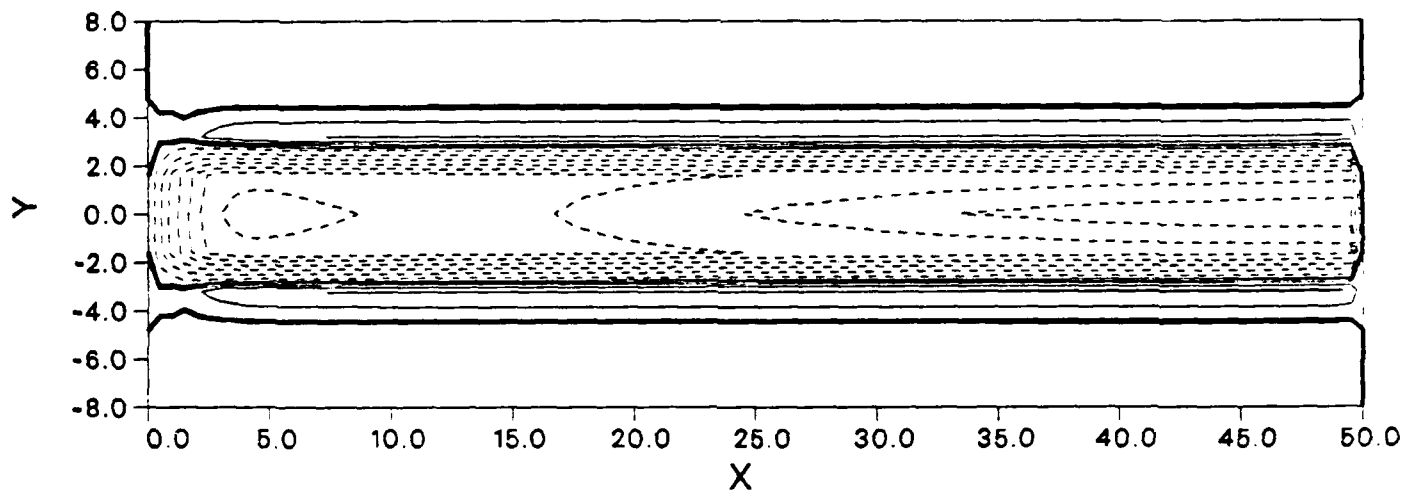
12

## U(X,Y), T=5 (INT.=0.002)



## U(X,Y), T=20 (INT.=0.02)



Figure 1: Zonal current anomaly. a) $t = 5$, contour interval = .002 m s$^{-1}$; b) $t = 20$, contour interval = .02 m s$^{-1}$. (Westward currents are dashed.)
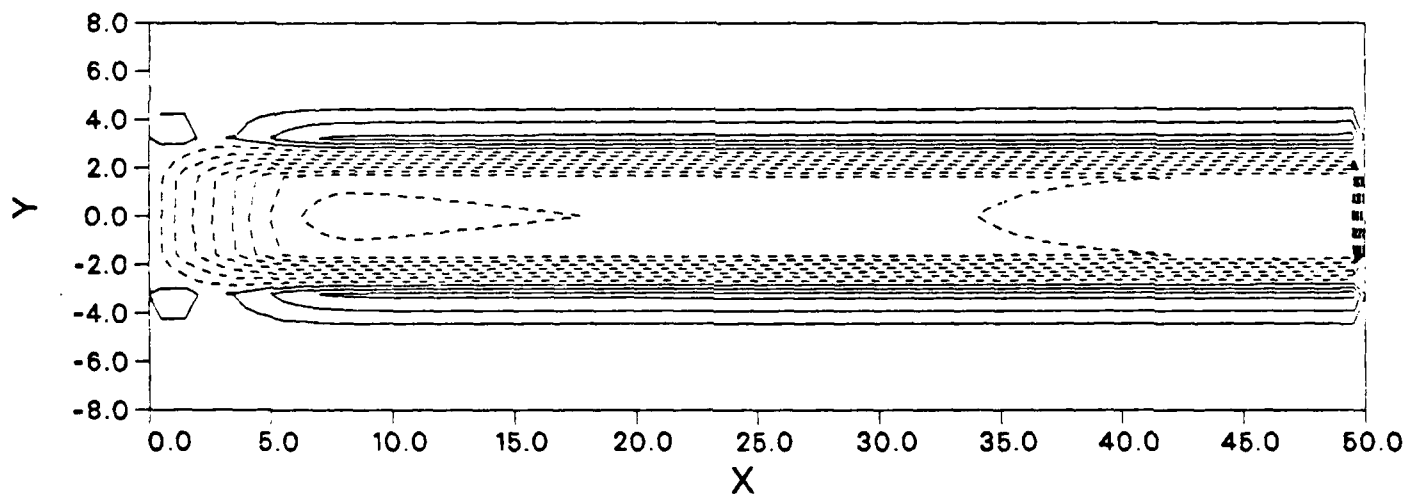
13

U(X,Y), T=50 (INT.=0.1)



U(X,Y), T=100 (INT.=0.2)



Figure 2: Zonal current anomaly. a) $t = 50$, contour interval $= .1$ m s$^{-1}$; b) $t = 100$, contour interval $= .2$ m s$^{-1}$.

14

one fourth of the basin, and higher order terms over successively smaller regions near the western boundary. This is to be expected, because of the slower phase speeds associated with the latter waves. However, since the magnitudes of the lowest order coefficients are much greater than those of the higher order terms, the qualitative character of the solution does not change significantly. The steady, basin-wide eastward wind stress results in a relative rise in sea level in the eastern part of the basin, and a westward equatorial flow with weak eastward return flow at higher latitudes.

## b Eastward moving pulse

The second case which was studied is more realistic, and therefore somewhat more complex. The wind stress is given by

$$\tau(t, x, y) = \left[1 - e^{-\alpha t}\right] \left[\Theta(x - \eta t) - \Theta(x - \lambda - \eta t)\right] A e^{-\frac{1}{2}\gamma v^2}$$

Thus, the surface stress is assumed to be in the form of an eastward moving pulse (top-hat) of anomalous westerly winds similar to that used by McCreary and Lukas (1986) in their study of an unbounded equatorial ocean. The zonal extent of the pulse ($\lambda$) is taken to be half the length of the basin ($\approx$ 7000 km) and it moves eastward with speed $\eta$ such that it traverses the basin in about 16 months. Its magnitude grows from zero to its asymptotic value with an exponential time constant of about four months. During this time, the leading edge of the pulse travels from the western boundary of the ocean to $x \approx 12$. The meridional shape and final magnitude of the forcing are the same as in the

15

zonally uniform case discussed above. This wind stress anomaly is more realistic than the uniform stress discussed in the previous section in that it is not zonally uniform, and the region of strongest anomalous wind stress propagates towards the east, eventually leaving the region. This behavior is not unlike the wind anomalies that are observed during major ENSO events such as 1982–83, and it is similar to that used by Blundell and Gill (1983) and McCreary and Lukas (1986).

The Laplace transform of the $n^{th}$ term of the Hermite expansion for $\tau(t, x, y)$ is

$$\hat{\tau}_n(s, x) = \left( \frac{1}{s} \left\{ 1 - e^{-sx/\eta} - \Theta(x - \lambda) \left[ 1 - e^{-s(x-\lambda)/\eta} \right] \right\} \right.$$
$$\left. - \frac{1}{s+a} \left\{ 1 - e^{-(s+a)x/\eta} - \Theta(x - \lambda) \left[ 1 - e^{-(s+a)(x-\lambda)/\eta} \right] \right\} \right) T_n$$

A particular solution to (17) with this forcing is

$$\hat{U}_n(s, x) = A_n(s) \left\{ P_n(s) + Q_n(s) e^{-sx/\eta} + R_n(s) e^{-(s+a)x/\eta} \right.$$
$$\left. - \Theta(x - \lambda) \left[ P_n(s) + Q_n(s) e^{-s(x-\lambda)/\eta} + R_n(s) e^{-(s+a)(x-\lambda)/\eta} \right] \right\}$$

where

$$A_n(s) = \beta^{-\frac{1}{2}} c^{-\frac{1}{2}} \left[ -\frac{1}{4} T_{n-2} + (s^2 + n + \frac{1}{2}) T_n - (n + 2)(n + 1) T_{n+2} \right]$$

$$P_n(s) = \frac{a}{s^2(s + a)(s^2 + 2n + 1)}$$

$$Q_n(s) = -\frac{\eta^2}{s^2[\eta^2(s^2 + 2n + 1) - \eta - s^2]}$$

$$R_n(s) = \frac{\eta^2}{(s + a)[s\eta^2(s^2 + 2n + 1) - (s + a)\eta - s(s + a)^2]}$$

16

Since $\hat{U}_n(s,x)$ is discontinuous at $x = \lambda$, the functions $f_n^\pm(s)$, discussed in Section 2, must be modified slightly to allow different solutions for $x < \lambda$ and $x \geq \lambda$. Additional boundary conditions require that the total solution, $\hat{u}_n(s,x)$, and its first derivative with respect to $x$ are continuous at $x = \lambda$.

The Hermite coefficients of the solution, $u_n(t,x)$, are shown in Figs. (3)–(7). Note that, in order to show details of the response, each figure has a different scale on the ordinate. The points at which the curves appear to be jagged (e. g. $u_0(50,x)$ for $x \approx 20$) correspond to points at which the numerical inversion of the Laplace transform failed to converge to the desired (1%) tolerance, and a 10% tolerance was accepted.

The dominance of the lowest order (Kelvin wave) term is clearly seen. Immediately after the pulse of eastward wind stress is initiated the $n = 0$ response retains the shape of the forcing, but propagates eastward at a considerably greater speed than does the prescribed forcing. This is the result of a superposition of a series of Kelvin waves, each propagating with speed $c$, which is about 5.6 times greater than the speed of the forcing, $\eta$. Once the leading edge of the Kelvin wave front reaches the eastern boundary ($t \approx 25 \approx 43$ days) the shape of the pulse is no longer preserved, due to reflections. The strongest response is seen at $t = 100$ ($\approx 170$ days). By $t = 200$, the leading edge of the forcing has moved beyond the eastern boundary of the ocean basin, so that only the eastern third of the basin is subject to direct forcing.

The $n = 2$ (Fig. 4) response is similar to that for $n = 0$, except that the leading edge of the response is retarded, due to the slower phase speed of the higher order wave mode.
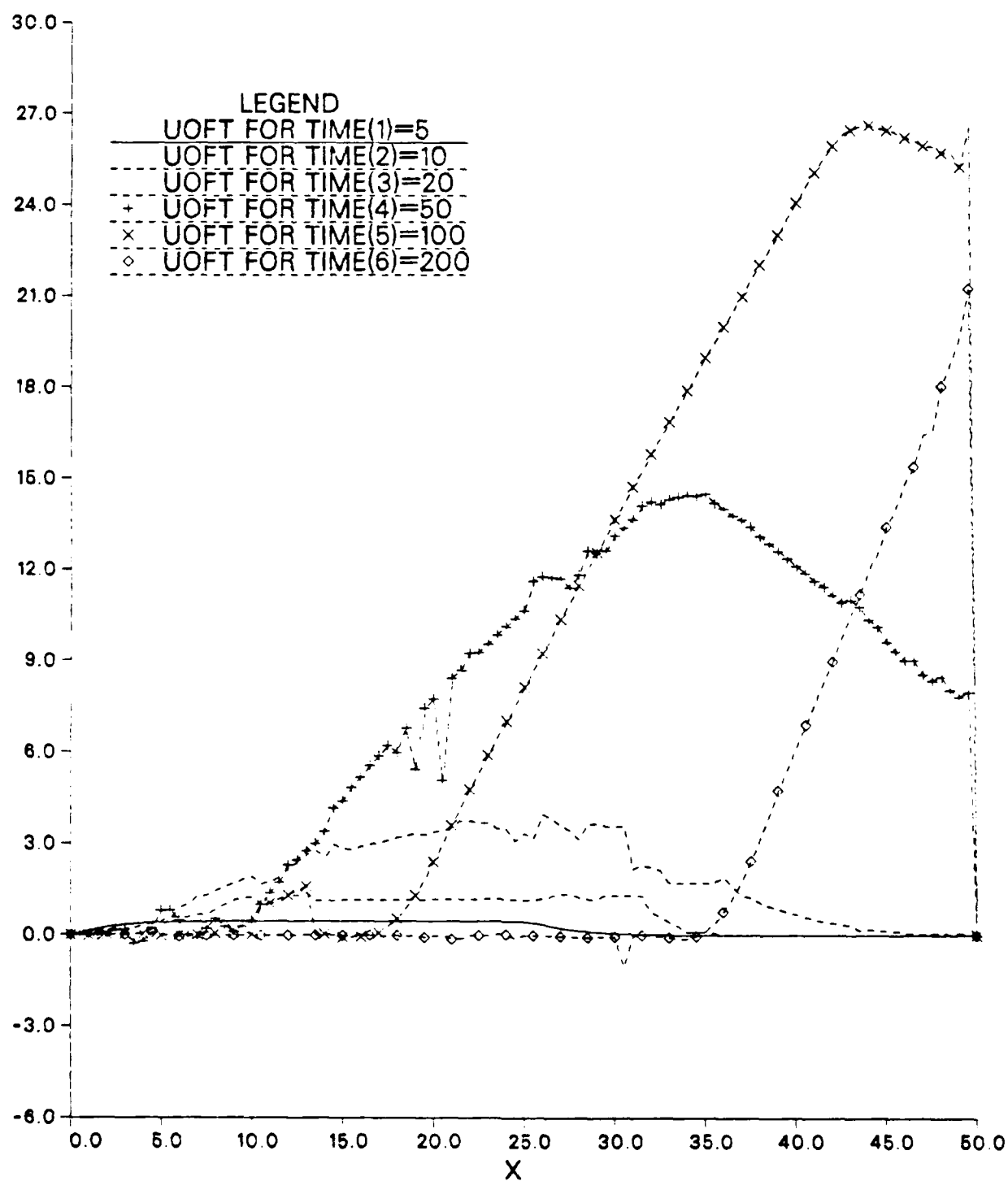
Figure 3: $u_0(t, x)$ vs $x$ (Vertical scale is m s$^{-1}\times$ 100)

18

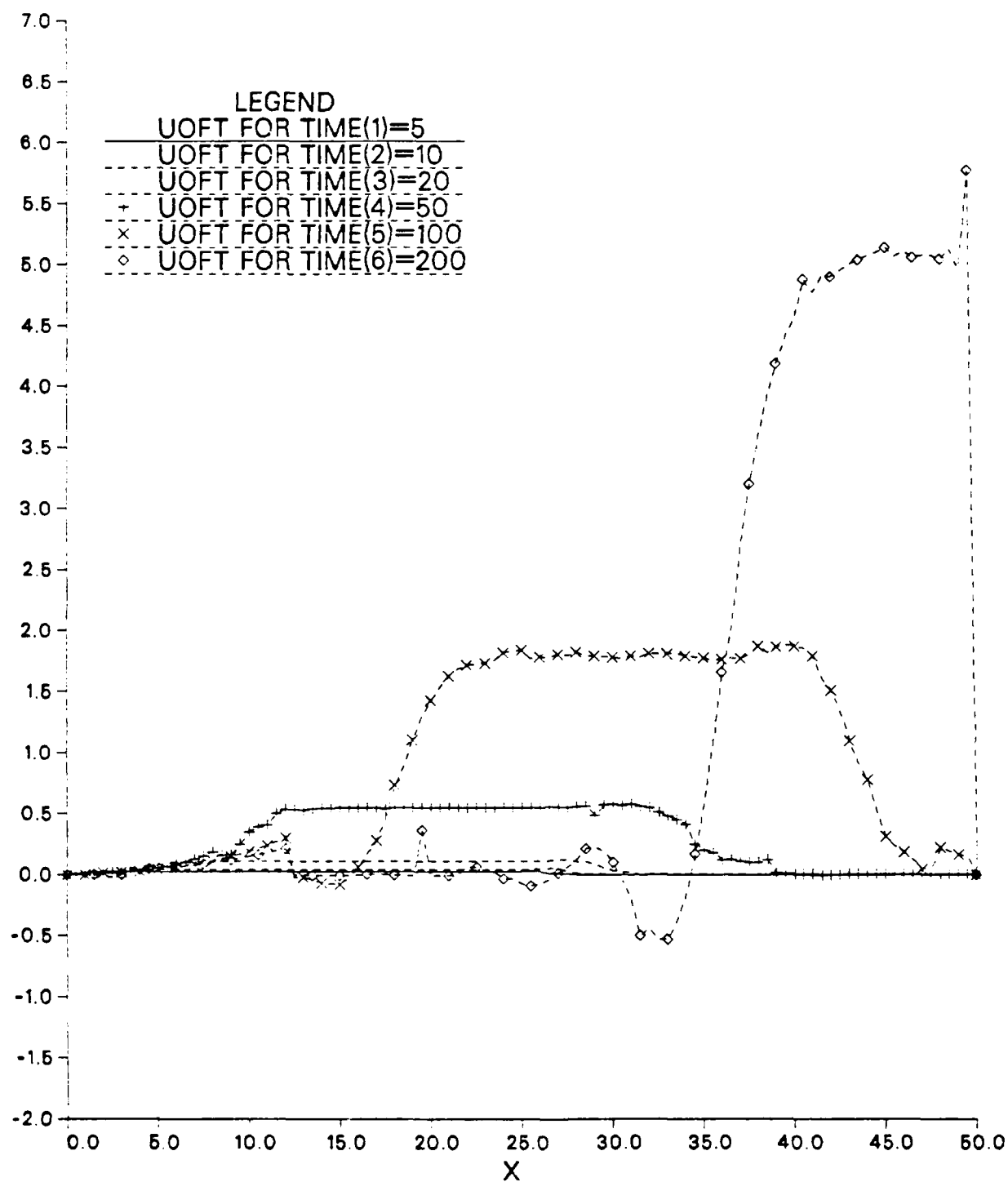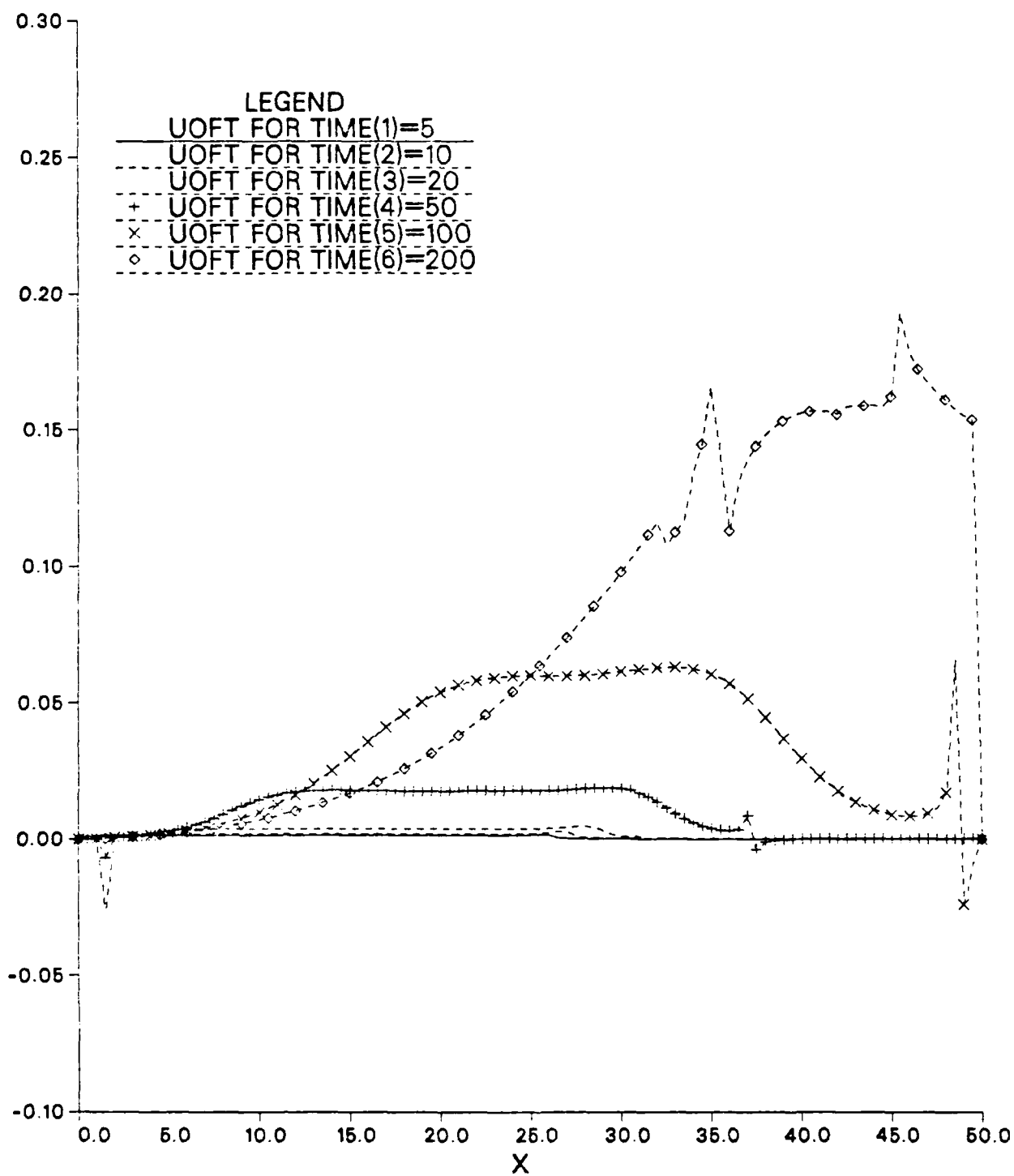Figure 4: $u_2(t, x)$ vs $x$ (Vertical scale is m s$^{-1}$ $\times$ 100)

19

Figure 5: $u_4(t,x)$ vs $x$ (Vertical scale is m s$^{-1}\times$ 100)

20

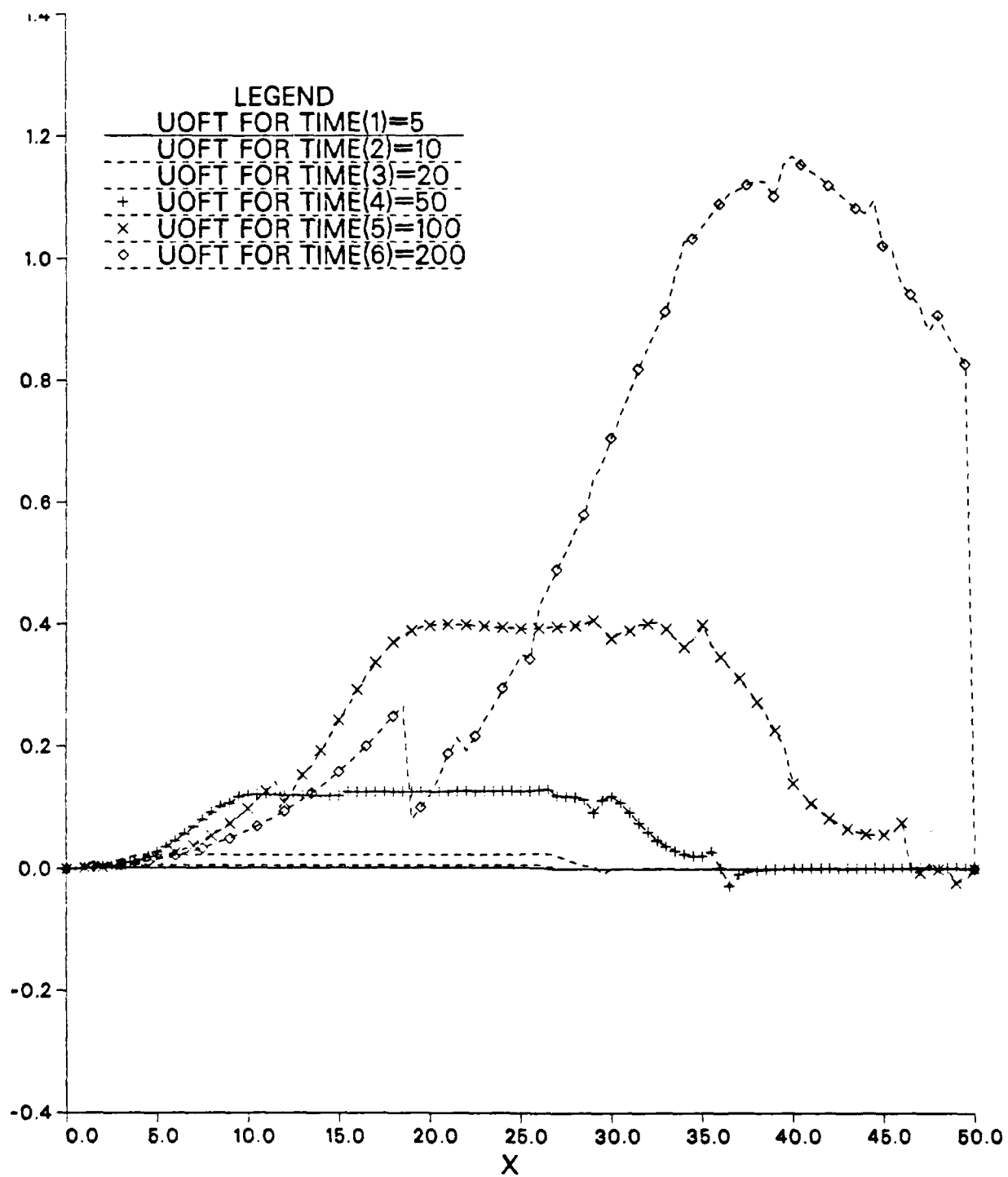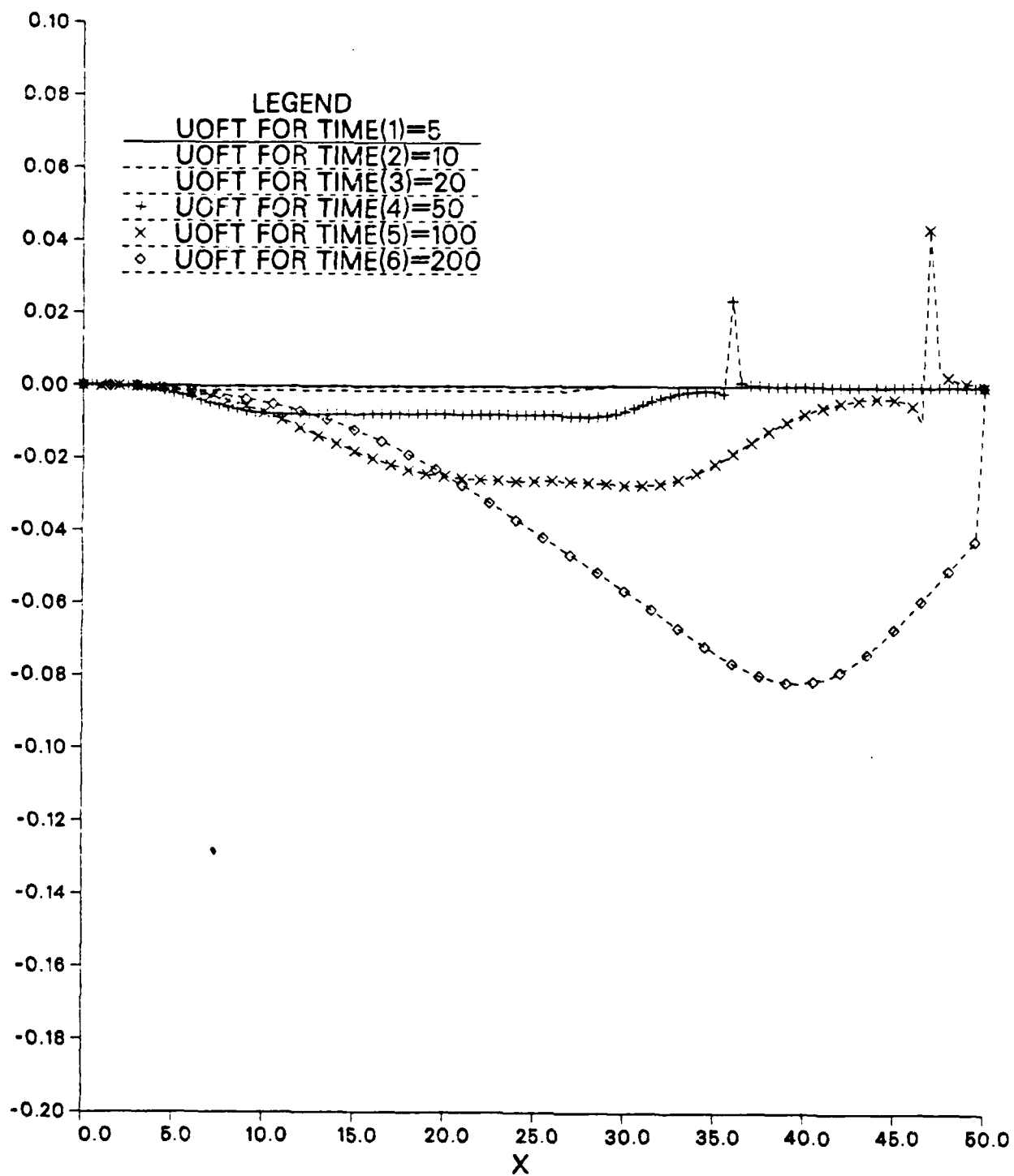Figure 6: $u_6(t, x)$ vs $x$ (Vertical scale is m s$^{-1}$ × 100)

21

Figure 7: $u_8(t, x)$ vs $x$ (Vertical scale is m s$^{-1}$ $\times$ 100)

22

The magnitude of the response is much smaller because the direct forcing of this mode is also much smaller. The higher order response (Figs. 5–7) follow this same pattern.

Even though the magnitude of the $n = 0$ term is considerably greater than that of the higher order modes, the latter have a distinct influence on the character of the complete solution. Fig. 8 shows the total zonal current anomaly at $t = 5$ and $t = 50$. As might be expected the initial response of the western part of the basin is rather similar to that found for the uniform forcing case. The currents are weaker, because the forcing approaches its final value more slowly, but the basic structure of westward currents at at the equator, flanked by eastward return flow, is the same. At $t = 5$, the leading edge of the forcing is at $x = 25.9$. The Kelvin wave front is at $x = 30$. To the east of $x = 30$ there is no disturbance, as the signal has not yet reached this region. By $t = 50$, the leading edge of the forcing has reached $x \approx 35$. To the west of this point, the solution still resembles that of the earlier case. However, evidence of the trailing edge of the forcing begins to appear in the far western part of the basin. Just ahead of the leading edge of the wind, a burst of eastward motion (a Kelvin wave front) exists, with only a weak response near the eastern boundary.

At later times (Fig. 9) the effect of the nonuniform, transient nature of the forcing becomes more pronounced. At $t = 100$ moderate ($\approx 1$ m s$^{-1}$) westward currents dominate the center of the basin. These currents decrease more rapidly towards the west than in the previous case (see Fig. 2) because the forcing there has vanised. The Kelvin wave front of strong eastward currents ahead of the forcing pulse has gained strength, and now extends
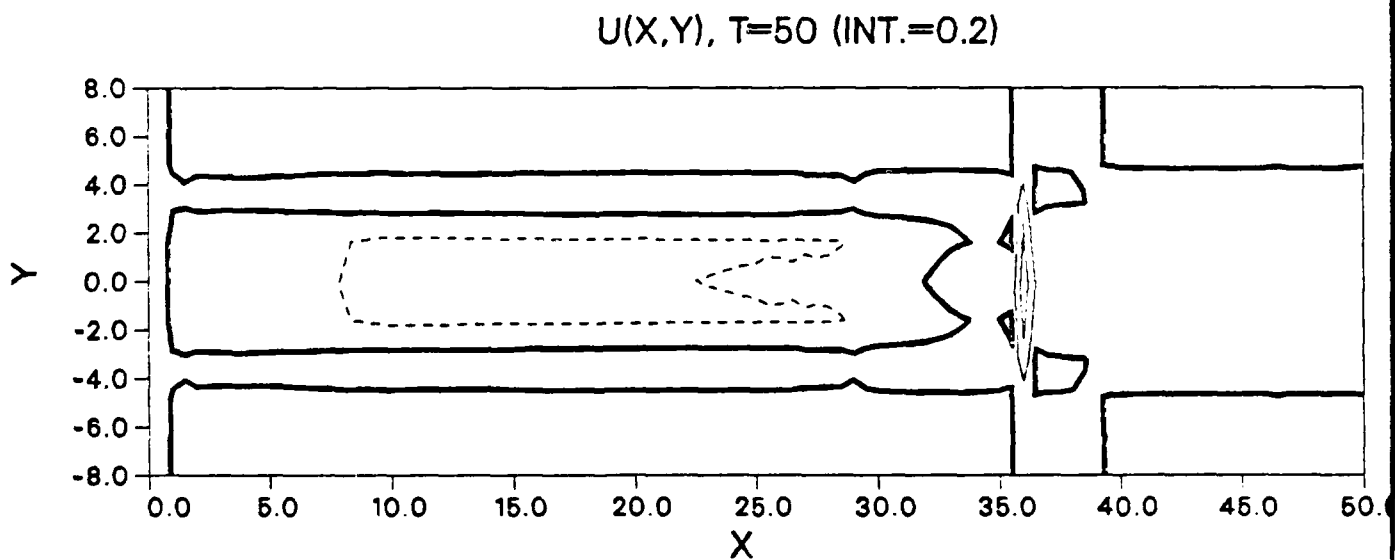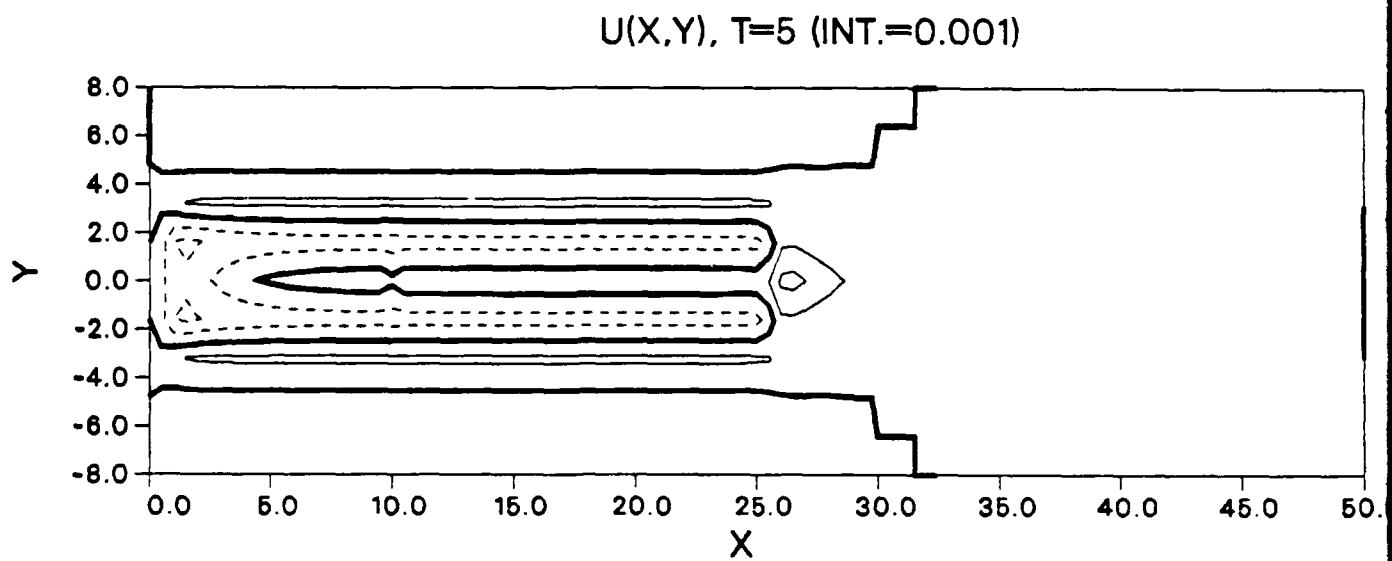
U(X,Y), T=5 (INT.=0.001)



U(X,Y), T=50 (INT.=0.2)



Figure 8: Zonal current anomaly. a) $t = 5$, contour interval $= .001$ m s$^{-1}$; b)$t = 50$, contour interval $= .2$ m s$^{-1}$
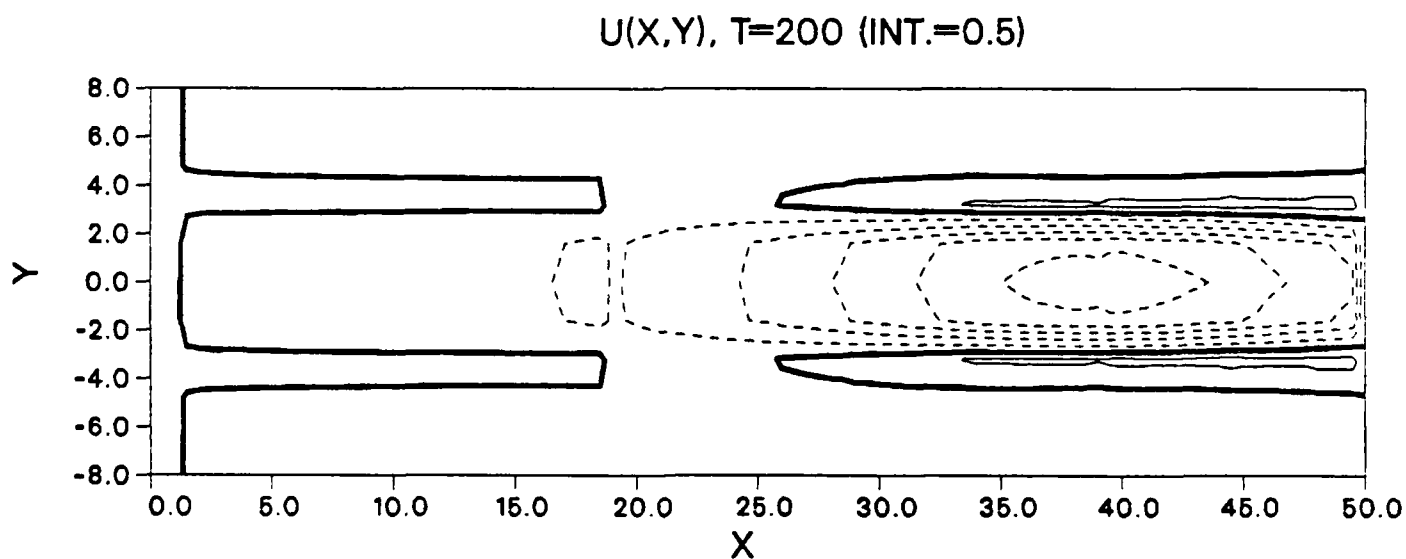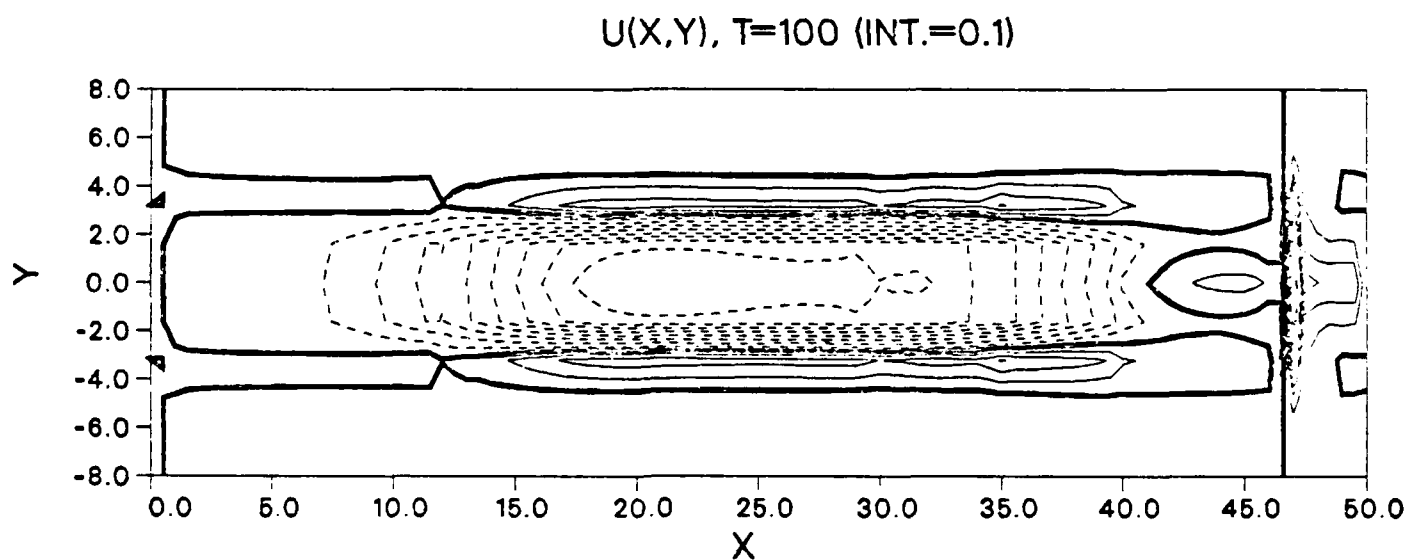
U(X,Y), T=100 (INT.=0.1)



U(X,Y), T=200 (INT.=0.5)



Figure 9: Zonal current anomaly. a) $t = 100$, contour interval $= .1$ m s$^{-1}$; b)$t = 200$, contour interval $= .5$ m s$^{-1}$

a considerable distance in the meridional direction. By $t = 200$ ($\approx 11$ months), only the eastern third of the basin is directly influenced by the forcing. There, the strong westward currents persist near the equator, with eastward flow to the north and south. To the west of the active forcing region, the flow is weaker.

At still later times (Fig. 10) the pulse of anomalous wind stress has exited the model ocean basin. For $t > 380$, the forcing vanishes across the entire basin. The current anomalies which persist are due to reflections of the waves which were generated as the forcing traversed the basin. Because the model includes no dissipation, these waves will persist for all time, but the shape of the disturbance will continue to fluctuate as the different wave modes superpose in different ways. At $t = 400$ the region of westward flow has expanded to fill almost the entire basin; the familiar bands of eastward flow have all but vanished. While this is not a strictly steady state configuration, the general state persists through $t = 500$, with only small qualitative changes due to the slow phase speeds of the higher order modes which dominate at this time.
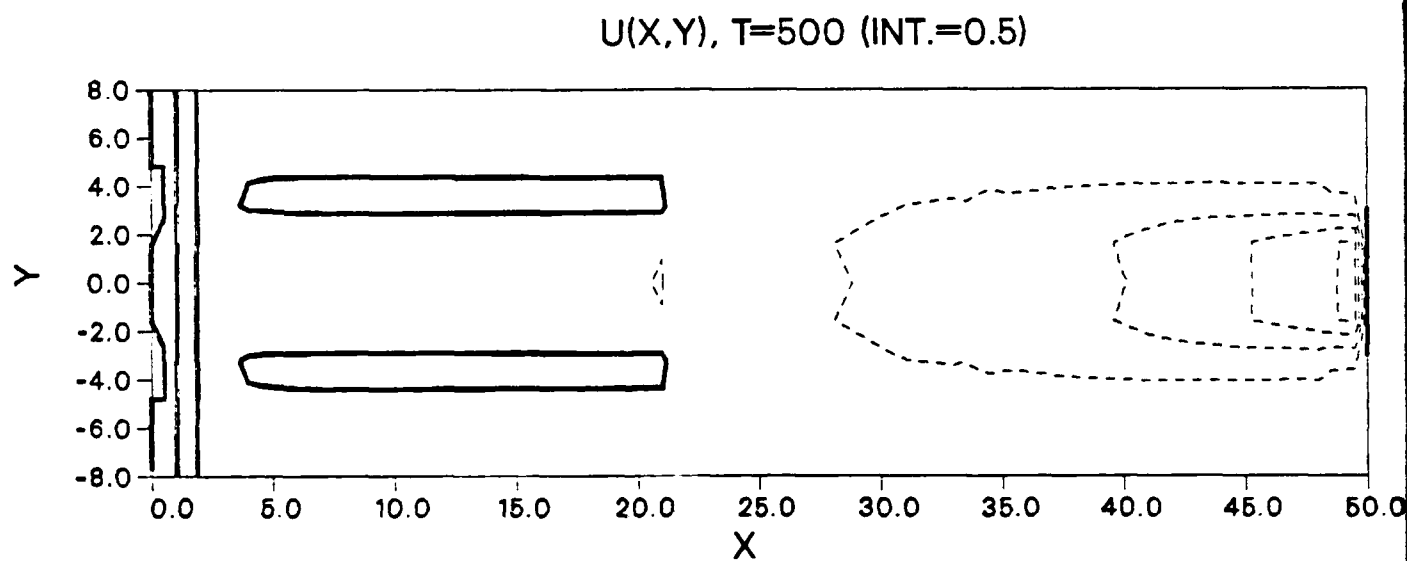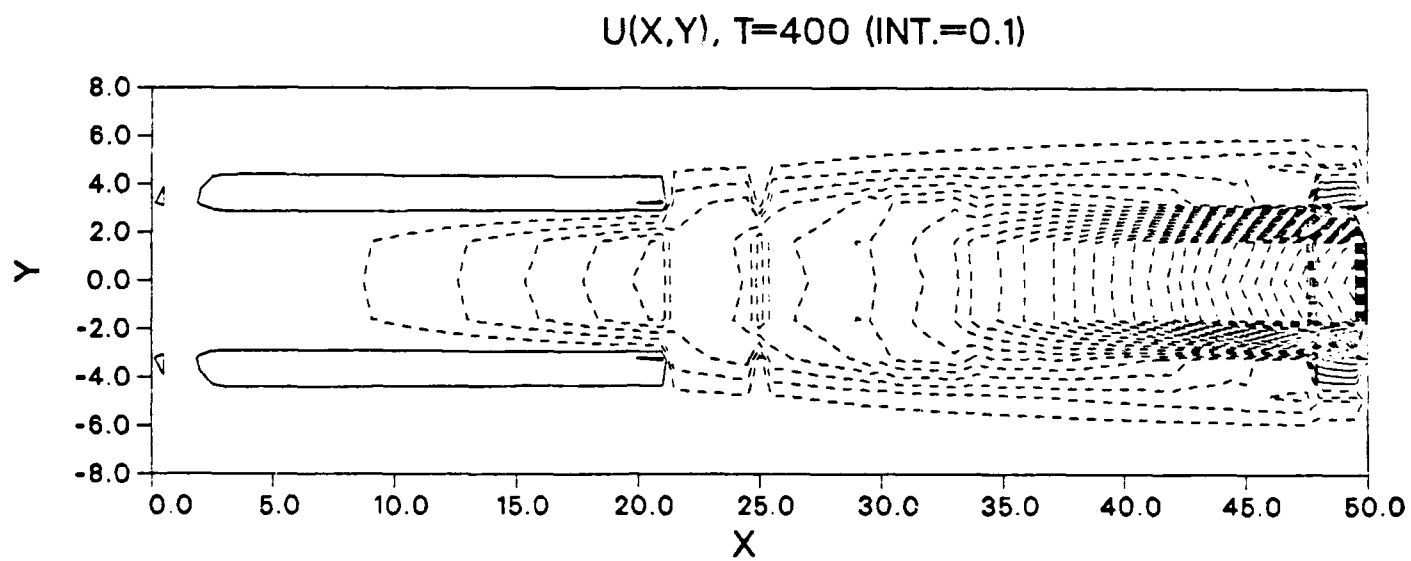
U(X,Y), T=400 (INT.=0.1)



U(X,Y), T=500 (INT.=0.5)



Figure 10: Zonal current anomaly. a) $t = 400$, contour interval = $.1$ m s$^{-1}$; b)$t = 500$, contour interval = $.5$ m s$^{-1}$

27

# 4 Sumary and Conclusions

In this report we have presented the analytic solution to the shallow water equations in a closed basin subject to arbitrary wind forcing. Two physically realistic example solutions were shown and interpreted in some detail. One example corresponded to the spin up of an equatorial ocean basin to a zonally uniform westerly wind anomaly. The other example was the transient response of the basin to a zonally oriented top-hat wind pulse that moved across the basin in a period of 16 months. This represented the wind forcing of an idealized version of the atmospheric Southern Oscillation.

The analytic solution resembles published results for an ocean basin (e. g. Cane (1979); Busalacchi and O'Brien (1981); Weisburg and Tang (1983)) which until now were obtained only using numerical models. Although our results are somewhat incomplete without the rest of the solution (i. e. $v$ and $h$), it is clear that the present analytic solution offers considerable potential for interpreting observations and numerical model results in equatorial oceanography.

# References

Blundell, J. R. and A. E. Gill, 1983: Equatorial ocean response to wind forcing. *Ocean Modeling*, **53**, 10-11.

Busalacchi, A. J. and J. J. O'Brien, 1981: Interannual variability of the equatorial Pacific in the 1960's. *J. Geophys. Res.*, **176**, 10901-10907.

Busalacchi, A. J., K. Takuchi, and J. J. O'Brien, 1983: Interannual variability of the equatorial Pacific–revisited. *J. Geophys. Res.*, **178**, 7551-7562.

Cane, M. A. 1979: The response of an equatorial ocean to simple wind stress patterns. *J. Mar. Res.*, **37**, 233-252 .

Cane, M. A., and E. S. Sarachik, 1976: Forced baroclinic ocean motions: I. The linear equatorial unbounded case. *J. Mar. Res.*, **34**, 629-665 .

Cane, M. A., and E. S. Sarachik, 1981: The response of a linear baroclinic equatorial ocean to periodic forcing. *J. Mar. Res.*, **39**, 651-693 .

Gill, A. E. 1980: Some simple solutions for heat induced tropical circulations. *Quart. J. Roy. Meteor. Soc.*, **106**, 447-462 .

Hirst, A. C. 1986: Unstable and damped equatorial modes in simple coupled ocean-atmosphere models. *J. Atmos. Sci.*, **43**, 606-630 .

Hirst, A. C. 1988: Slow instabilities in tropical ocean basin-global atmosphere models. *J. Atmos. Sci.*, **45**, 830-852 .

Hurlburt, H. E. , J. C. Kindle and J. J. O'Brien 1976: A numerical simulation of the onset of El Nino. *J. Phys. Oceanogr.*, **6**, 621-631 .

Lau, K. M. 1981: Oscillations in a simple equatorial climate system. *J. Atmos. Sci.*, **38**, 248-261 .

McCalpin, J. D. 1988: A note on the reflection of low-frequency equatorial Rossby waves from realistic western boundaries. *J. Phys. Oceanogr.*, **17**, 1944-1949 .

McCreary, J. P., 1976: Eastern tropical ocean response to changing wind systems: With application to El Nino. *J. Phys. Oceanogr.*, **6**, 632-645 .

McCreary, J. P., and R. Lukas, 1986: The response of the equatorial ocean to a moving wind field. *J. Geophys. Res.*, **91**, 11691-11705 .

Philander, S. G. H. , T. Yamagata and R. C. Pacanowski, 1984: Unstable air-sea interactions in the tropics. *J. Atmos. Sci.*, **41**, 604-613 .

Rennick, M. A., 1983: A model of atmosphere-ocean coupling in El Nino. *TO-AN*, **15**, 2-4 .

Rennick, M. A. and R. L. Haney, 1986: Stable and unstable air-sea interactions in the equatorial region. *J. Atmos. Sci.* , **43**, 2937-2943.

Schopf, P. S. and M. J. Suarez, 1988: Vacillations in a Coupled Ocean-Atmosphere Model. *J. Atmos. Sci.*, **45**, 549-566.

Weisburg, R. H., and T. Y. Tang, 1983: Equatorial ocean response to growing and

moving wind systems with application to the Atlantic. *J. Mar. Res.*, **41**, 461-4867 .

White, W. B., G. A. Meyers, J. R. Donguy, and S. E. Pazan, 1985: Short term climatic variability in the thermal structure of the Pacific Ocean during 1979–82. *J. Phys. Oceanogr.*, **15**, 917-935 .

Yamagata, T., 1985: Stability of a simple air-sea coupled model in the tropics. *Coupled Ocean-Atmosphere Models*, J. C. J. Nihoul, ed., Elsevier, Amsterdam, 767pp .

# Report Distribution